

## Assessing Liquefaction Potential in Alluvial Plains Through Spatiotemporal Analysis Using Liquefaction Probability Index

Badr Berkat <sup>1\*</sup>, Ahmed Akhssas <sup>1</sup> , Omar Elfilali <sup>1</sup>

<sup>1</sup> *Laboratory of Applied Geophysics, Engineers Geology, Geotechnical and Environmental Sciences, Mohammadia School of Engineers, Mohammed V University in Rabat, Avenue Ibn Sina, Agdal, Rabat and 10090, Morocco.*

Received 06 February 2024; Revised 25 April 2024; Accepted 11 May 2024; Published 01 June 2024

### Abstract

Liquefaction is one of the most important processes in soil dynamics. It is a loss of strength coupled with a rapid increase in pore pressure, causing soil particles to burst for a short period. Several approaches have been developed to calculate the residual or liquefied shear strength of cohesionless soils. Using the liquefaction probability index (LPI) created by Juang et al. (2003), the primary goal of this publication is to map spatiotemporal variations in the liquefaction potential of deposits in the Oued Drader and Marja Zerga alluvial plains of the mio-plio-quadernary Gharb basin. The cone penetration test (CPT) and semi-empirical techniques developed to measure the risk of liquefaction and create a mapping of liquefiable zones on a national scale for the first time are the primary sources of information used in the computation of the liquefaction potential index (LPI), which will be highly applicable and relevant for upcoming research projects. According to the IPL calculation, liquefaction is expected to be confirmed for the sandy and silty-sandy formations in Oued Drader and Marja Zerga. The spatial-temporal variations will depend on the formation's granulometry, saturation level, and liquidity limit. The lateral and spatial variety of the Marja Zerga and Oued Drader plain deposits is reflected in this architecture of liquefaction variation.

*Keywords:* Liquefaction Probability Index; Dense Ground; CPT.

### 1. Introduction

One of the most complex and dangerous phenomena in the dynamics of mobile soils in extremely seismic zones is liquefaction. This phenomenon affects geological formations with low compaction and small, uniform grain sizes, such as clays, sands, and silts. The effects of soil liquefaction as a function of specific seismic intensity have been studied by several researchers to assess the potential for liquefaction [1–4]. Semi-empirical methodologies have been developed using theoretical considerations and experimental data, including in situ testing, to calculate the liquefaction probability index (LPI) [4–7]. These semi-empirical methods fall into three categories: (i) the cyclic stress approach, (ii) the cyclic strain approach, and (iii) the energy approach. The cyclic stress approach is the most established and commonly utilized in practice, and it is based on calculating the ratio of cyclic stress to cyclic resistance [1–4, 8].

Morocco is a country known for its geological and geotechnical peculiarities and seismic activity. Consequently, and particularly in the study area, geotechnical studies based on dynamic static cone penetrometer (CPT) tests [1, 2, 9, 10] were carried out to assess the liquefaction potential of the area located in the Oued Drader and Marja Zerga alluvial plain, with the aim of calculating a liquefaction probability index (LPI) using semi-empirical methods. According to previous research [4, 11, 12], the method used in our investigation, as well as that of Juang et al. [4], offers the best

\* Corresponding author: [badr\\_berkat@um5.ac.ma](mailto:badr_berkat@um5.ac.ma)

 <http://dx.doi.org/10.28991/CEJ-2024-010-06-018>



© 2024 by the authors. Licensee C.E.J, Tehran, Iran. This article is an open access article distributed under the terms and conditions of the Creative Commons Attribution (CC-BY) license (<http://creativecommons.org/licenses/by/4.0/>).

compromise for assessing liquefaction potential in this study, as it is based on a very robust physical component. In addition, Juang used an artificial neural network formulation. Furthermore, the method is both reassuring and less sensitive to uncertainties that may have an impact on soil properties [7, 11-13].

Before embarking on the detailed calculation of the Liquefaction Probability Index (LPI), two methodological approaches were used: In a preliminary study, it is possible to determine whether the soil is susceptible to liquefaction by first using theoretical criteria based on local geological, morphological, and hydrological data and then using the peak resistance measured by the CPT test and determined as a function of depth. Accordingly, and to filter out the large amount of data, we processed all boreholes using the following rule of thumb: geological formations with peak resistance  $q_c$  of the order of 5000 kPa and above, meaning that the effective stress is quite considerable compared to the pore pressure, indicating that the soil is compact and not dense enough to be susceptible to liquefaction [14].

The results of LPI calculations confirm liquefaction with spatial-temporal fluctuations, particularly for drill holes bordering Oued Drader and Merja Zerga, given the degree of saturation, the granulometry, and the nature of the formations, which are not compact at certain depths.

## 2. Regional Data

### 2.1. Geology

The primary sedimentary series in the plio-quaternary aquifer complex of the Gharb basin are sandy sandstone formations, with numerous abrupt lateral and vertical changes in the sedimentary layers [15, 16]. The study area is mostly made up of alluvial deposits, which include clay, water-bearing silts, fine and coarse sand layers, and semi-permeable silt. The soils in this area are heavily influenced by the textural nature of the bedrock, which is made up of Quaternary sands (Figure 1) [15, 16].

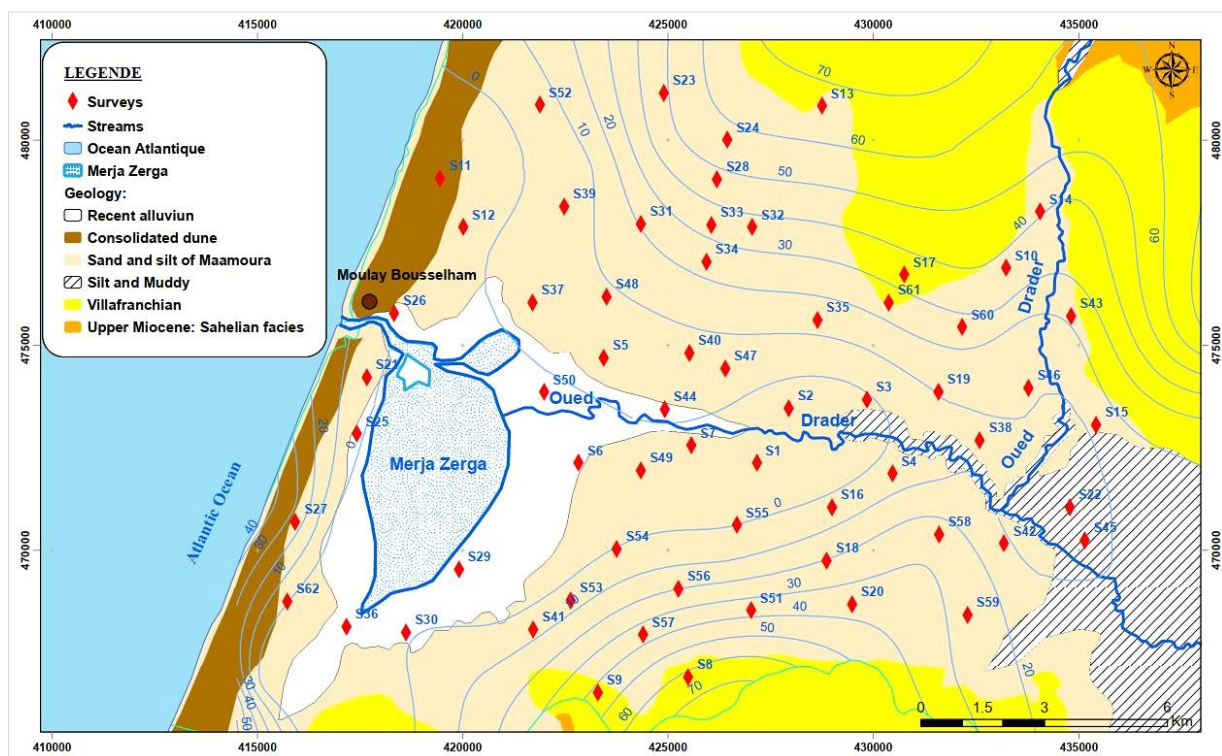


Figure 1. Geological map of the study area (Modified 1:200,000 geological map of Gharb and Prérif Occidental, 1952)

### 2.2. Hydrogeology

The Drader-Souire basin is currently one of eleven Sebou sub-basins. It is located north of the Gharb plain, between Kenitra and Larache, on the Atlantic coast. The basin is distinguished by its undulating terrain and sandy soils [15–17].

According to historical piezometric maps, the basin has three zones. According to Killi et al. [15] and Aberkane [16], two places lack a significant aquifer, including the Merja Zerga lagoon with saline water. The Drader-Souire basin has two aquifer units separated by sandy-clay or clay formations that act as a semi-permeable barrier and are correlated with the Villafranchian.

### 2.3. Geomorphology

The Drader-Souiere basin is bowl-shaped, with gradually decreasing slopes from the surrounding hills to the basin floor and the coastal Merjas along the inland sand dunes [18]. Information on geomorphological units can be used as a source of data to assess liquefaction potential in the study area. They have been classified (see Table 1) according to their liquefaction potential [19, 20].

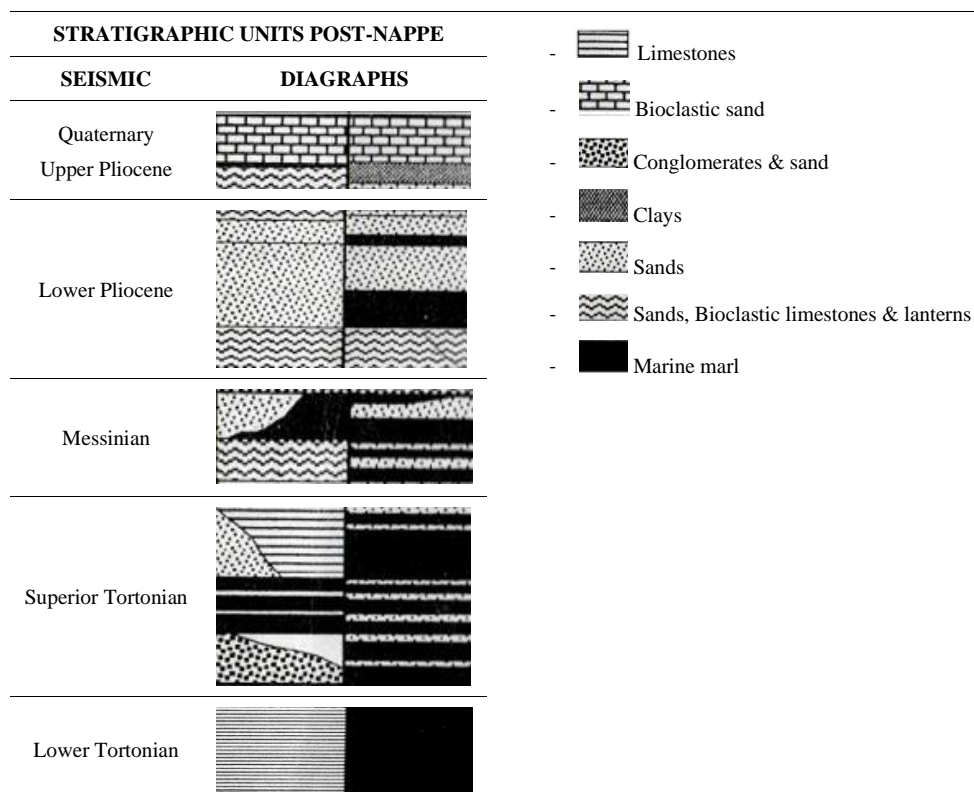
**Table 1. Liquidity potential classification based on morphological units [19]**

Rank	Geomorphologic Units	Potential liquefaction
A	Resent Riverbed, Old Riverbed, Swamp, Reclaimed Land, and Interdune Low	Liquefaction likely
B	Fan, Natural Levee, Sand Dune, Flood Plain, Beach, and Other Plains	Liquefaction possible
C	Terrace, Hill and Mountain	Liquefaction not likely

### 2.4. Stratigraphy

Information on a stratigraphic chart Sands with silt and clay passages, as well as biological zones, characterize the study area. The lithological texture of these deposits ‘ranges from the edge to the center of the Drader-Souiere basin, with a total thickness of more than 2,000 m. They form a dense sequence of marl and clay (Table 2). They are made up of sedimentary strata, which consist of thick clayey-silty open sea levels, indicating a deltaic and turbid environment [21–23].

**Table 2. Modified stratigraphic column of the Gharb basin [23]**



### 2.5. Seismicity of the Area

Morocco is vulnerable to major earthquakes due to its location in a continental collision zone and the proximity of African and European tectonic plates. At the level of the Drader-Souiere fault, the maximum intensity is around VII, but given that the zone is in critical seismic zones, including a historical earthquake site, the maximum intensity is IX, which is considered a non-negligible intensity (Figure 2). If we consider the worst-case scenario, a magnitude of M=7 is maintained due to the recent earthquake in Morocco [24].

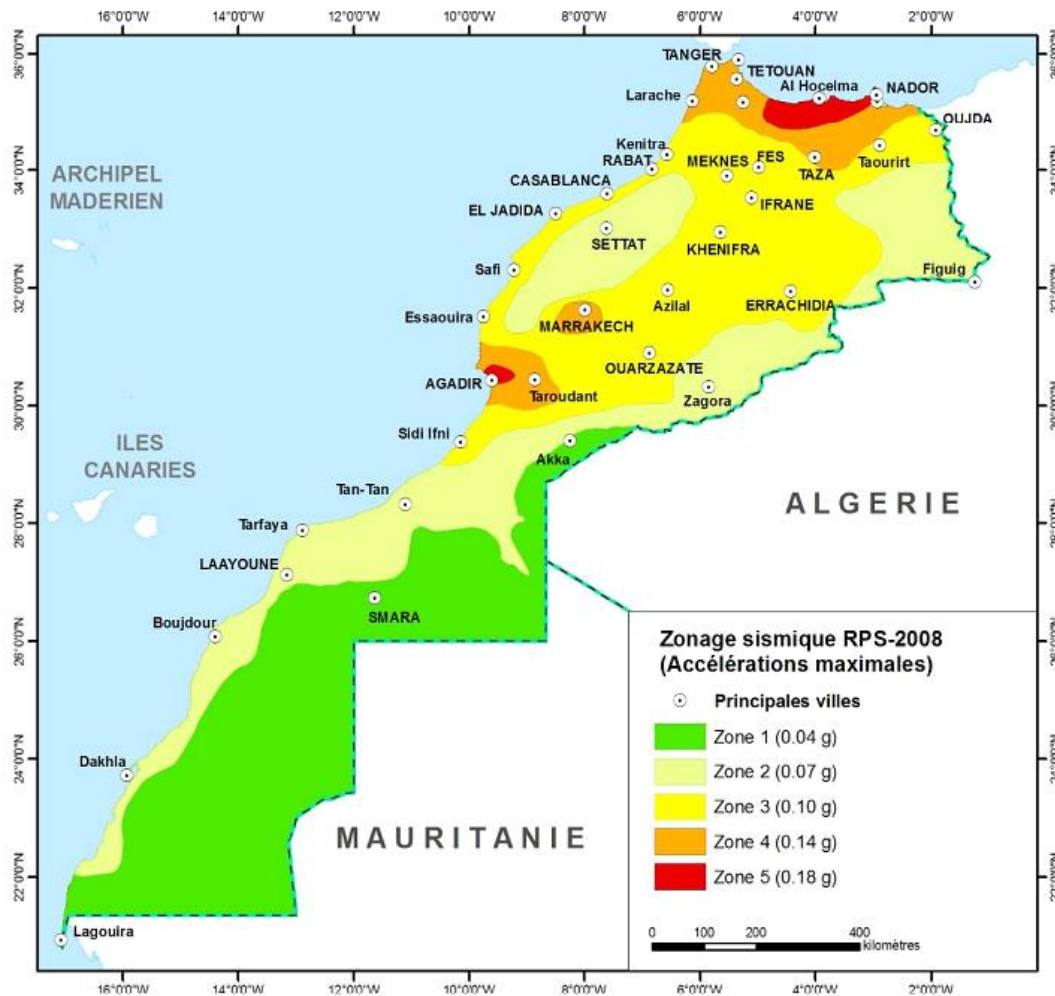


Figure 2. Seismic zoning in Morocco [24]

### 3. Material and Methods

In the analysis of liquefaction potential, two variables are generally used: (i) the soil's resistance to liquefaction, also known as the cyclic resistance ratio (CRR), and (ii) the cyclic stress ratio (CSR), which is the cyclic stress caused by an earthquake divided by the effective vertical stresses of the overburden. The CRR index, which reflects the soil's resistance to cyclic loading, frequently induced by an earthquake, is compared with the CSR when analyzing liquefaction potential. Liquefaction only occurs when the safety factor is less than unity [1, 8, 25].

The steps for estimating the liquefaction potential are the following:

- Check that the material is saturated;
- Verification of initial ground conditions to determine whether there is a possibility of liquefaction in the first place;
- Check that the energy released by earthquakes is capable of causing liquefaction;

Take account of actual seismic magnitudes by calculating the MSF factor;

- Calculation of the equivalent normalized cyclic shear stress (CSR) by coefficient  $r_d$  for each depth;
- Calculation of normalized cyclic shear strength CRR;
- Calculation of the factor and correction of the safety factor ( $FS = (CRR * MSF) / CSR$ );
- Final calculation of the safety factor for all depths with an interval of 0.1 meters;
- Plotting of safety factor curves as a function of depth.

This logic can be described as the following flow chart (Figure 3):

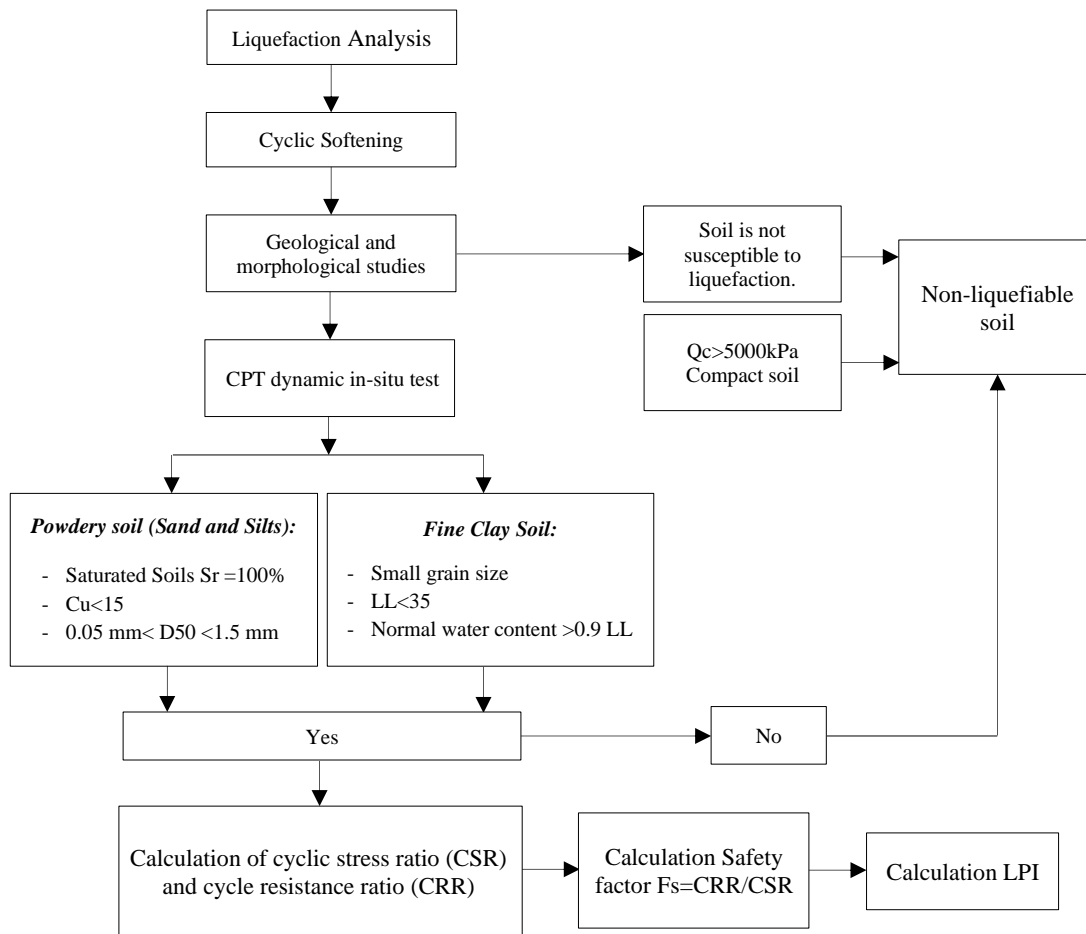


Figure 3. Flowchart of the methodology

### 3.1. Evaluation of the Cyclic Stress Ratio (CSR) Caused by Earthquake

CSR is the mean cyclic shear stress in a layer ( $\tau_{av}$ ) normalized to the effective stress due to the overlying soil ( $\sigma'_v$ ), based on the condensed strategy proposed by Seed and Idriss (1971), who gave the following references [8, 26]. The estimation of CSR is as follows:

$$CSR = \frac{\tau_{av}}{\sigma'_{v0}} = 0.65 \left( \frac{a_{max}}{g} \right) \left( \frac{\sigma_{v0}}{\sigma'_{v0}} \right) r_d \tag{1}$$

The stress reduction coefficient is represented as a function of depth using the following equations [27].

$$r_d = 1 - 0.00765 Si \quad Z \leq 9.15 \text{ m} \tag{2.a}$$

$$r_d = 1 - 0.00765 Si \quad 9.15 \text{ m} \leq Z \leq 23 \text{ m} \tag{2.b}$$

Juang et al. [4] used Equation 1 to calculate the CSR, and the MSF coefficient was added to the equation to adjust the CSR value for a magnitude 7.5 earthquake.

$$CSR = \frac{\tau_{av}}{\sigma'_{v0}} = 0.65 \left( \frac{a_{max}}{g} \right) \left( \frac{\sigma_{v0}}{\sigma'_{v0}} \right) \frac{r_d}{MSF} \tag{3}$$

According to Idriss & Boulanger (2008) [3], MSF is expressed by Equation 4:

$$MSF = 10^{2.24} / M_W^{2.56} = \left( \frac{M_W}{7.5} \right)^{-2.56} \tag{4}$$

### 3.2. Cyclic Resistance Ratio (CRR) from Cone Penetration Test

Seed & Idriss [1] are developed a method that allows for a more objective derivation of the boundary curve, which is referred to as the limit state in this instance. The technique utilizes artificial neural networks that have been trained to deduce the link between input and output from a database containing field liquefaction performance data. The limit state is then established using the trained neural network. Juang et al. [4] carried out least-square regression studies of the

data points produced by the neural network to enable the application of the neural network-generated limit state. The following empirical equation was obtained:

$$CRR = C_{\sigma} \exp \left[ -2.957 + 1.264 \left( \frac{q_{e1N,es}}{100} \right)^{1.25} \right] \tag{5}$$

$$C_{\sigma} = -0.016 \left( \frac{\sigma'_{v0}}{100} \right)^2 + 0.178 \left( \frac{\sigma'_{v0}}{100} \right)^2 - 0.063 \left( \frac{\sigma'_{v0}}{100} \right) + 0.903 \tag{6}$$

$$q_{c1N,es} = K_I q_{e1N} \tag{7}$$

$$K_I = 2.249(I_c)^4 - 16.943(I_c)^2 - 51.497(I_c) + 22.802 \tag{8}$$

$$I_c = [(3.47 - \log_{10}(F) + (\log_{10} F + 1.22)^2)^{0.5}] \tag{9}$$

$$F = \frac{f_s}{(q_c - \sigma_v)} \times 100 \tag{10}$$

### 3.3. Assessment of Safety Factor (SF) and Liquefaction Probability Index (IPL)

The safety factor is expressed as follows [8, 26]:

$$F_s = \frac{CRR}{CSR} \tag{11}$$

The chance of liquefaction can be calculated using the safety factor [4, 11].

$$IPL = \frac{1}{1 + (F_s/A)^B} \tag{12}$$

Juang's technique gives values of A = 0.96 and B = 4.50.

Based on the probability index provided by Equation 12, the liquefaction occurrence class is shown (Table 3)[4].

**Table 3. Occurrence of liquefaction by probability index [11, 14]**

IPL	Class	Description (probability of liquefaction)
$IPL \geq 0.85$	5	Liquefaction almost certain
$0.65 \leq IPL < 0.85$	4	Liquefaction very likely
$0.35 \leq IPL < 0.65$	3	Moderate
$0.15 \leq IPL < 0.35$	2	Liquefaction unlikely
$IPL < 0.15$	1	Liquefaction almost impossible

## 4. Results and Discussion

Based on the results of the dynamic in situ tests, the mechanical characteristics measured in the laboratory and based on the geological and geographical data of the study area were considered. The specific explanatory variables selected to assess susceptibility to liquefaction are as follows:

- Geology, hydrogeology, and morphology of the study area:

Excavated boreholes provided a distribution of groundwater levels, which showed the existence of a water table from level 0 in some places, as shown on the piezometric map in figure 1. The liquefaction phenomenon may occur due to the distribution of loose sand layers containing shallow aquifers, in line with Touijrate et al. [13] findings on the Drader area, which confirmed that the geology and lithology of the terrain are susceptible to liquefaction.

On the other hand, and according to the data presented in Table 1, the geomorphological characteristics of the study area place it in the category where liquefaction is probable [13]. Table 4 summarizes the degree of susceptibility to liquefaction according to the characteristics of the study area.

**Table 4. Classification of liquefaction susceptibility according to macro-engineering parameters**

Sr. No.	Macro geo engineering Parameter	Liquefaction Potential	Category
1	Geology	Yes	Moderate - Very High
2	Geological age of sediments	Yes	Moderate - High
3	Water table depth	Yes	None - High
4	Geomorphology	Yes	Moderate - High
5	Seismicity	Yes	Low - High

- Mechanical testing:

The depths most affected by liquefaction are those between 6 and 14 m, with high liquefaction probabilities for silty and sandy soils of the “silty sands to sandy silts” type where the IPL exceeds 0.90, specifically for boreholes located along the Oued Drader and Merja Zerga riverbeds, according to an analysis of CPT test data from the various drilled boreholes. Our study's findings are entirely consistent with those of Toujrate et al. [13].

IPL calculations show that, due to their grain size (Figures 4 and 5), sand and silty sand formations are the most susceptible to liquefaction, while other formations are moderately to slightly liquefied. Clay layers, on the other hand, are not at risk.

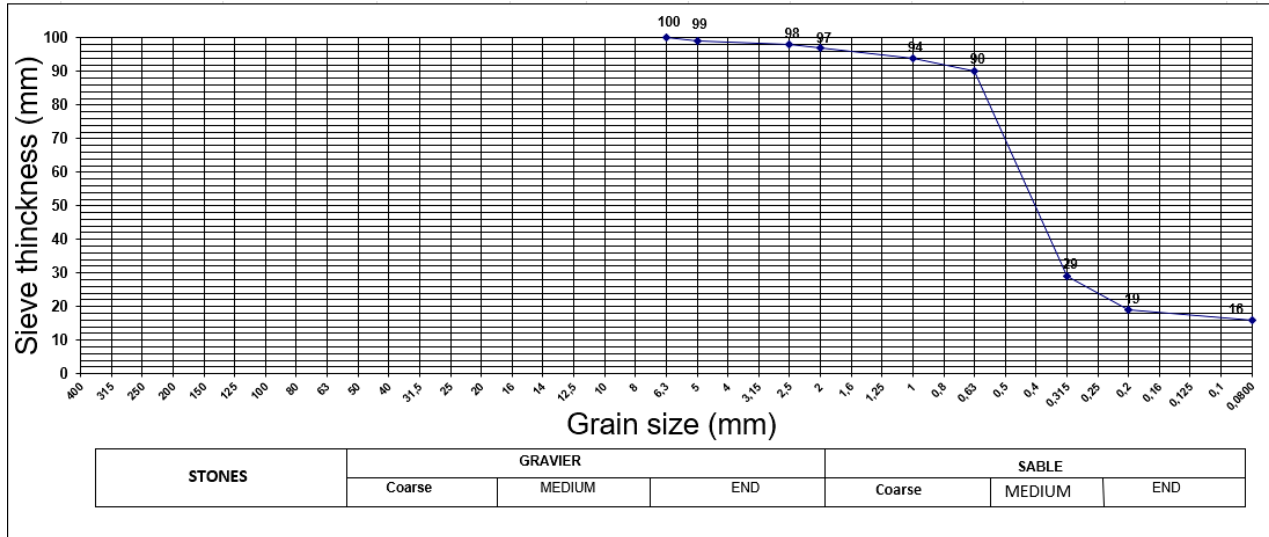


Figure 4. Sieve size curve for drill hole 1

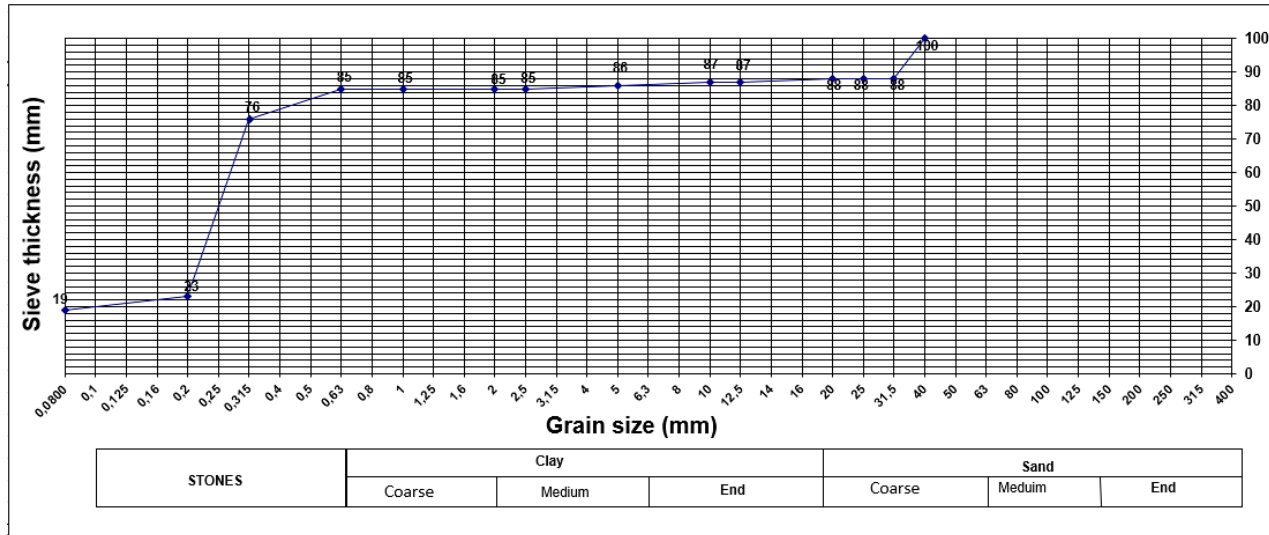


Figure 5. Sieve size curve for drill hole 4

The calculation of the liquefaction probability index (IPL) indicates a high probability of liquefaction along the Oued Drader alluvial plain and the Merja Zerga fluvial plain in the sand, silt, sandy-clay, silty-clay, and soft-clay layers (Table 5). Liquefaction maps were drawn up at depths of -7 m, -14 m, and -21 m to assess the different spatial-temporal variations in liquefaction of the Drader-Souiere and Merja Zerga alluvial plain formations.

The results of the calculations show that the probability of liquefaction in the drills lies at the edge of the Oued Drader alluvial plain and the Marja Zerga river plain (Table 5 and Figure 6). At a depth of -7m, certain to very probable liquefaction is limited to the Marja Zerga level and along the Oued Drader. This suggests that the proximity of the Merja Zerga may influence soil susceptibility to liquefaction at this depth, especially in the sandy, silty, and sandy-clay layers.

Table 5. Calculating Fs, IPL, and ROC

Drill	Soil type	Depth. (m)	$\sigma'p$ (kPa)	$\sigma'v_0$ (kPa)	Roc = $\sigma'p / \sigma'v_0$	FS	IPL	Liquefaction potential	Over-consolidation ratio
S1	Soft clay silt	0 to 7	17	192	0.1	0.88	0.63	Moderate	Under-consolidated
	Clayey sand and sandy silt	7 to 14	65	220	0.3	0.49	0.94	almost certain	Under-consolidated
	Loamy sand and weathered sandstone	14 to 22	150	338	0.4	0.70	0.81	very likely	Under-consolidated
S11	Sand to silty sand	0 to 7	220	168	1.3	1.3	0.07	Almost impossible	Over-consolidated
	Sandy Clay	7 to 14	250	160	1.6	1.6	0.02	Almost impossible	Over-consolidated
	Clayey silt and soft clay	14 to 22	150	120	1.3	1.3	0.06	Almost impossible	Over-consolidated
S14	Sand and silt	0 to 7	40	218	0.2	0.77	0.73	very likely	Under-consolidated
	Clayey sand and sandy silt	7 to 14	10	200	0.1	0.85	0.63	Moderate	Under-consolidated
	Sandy clay marl	14 to 22	150	170	0.9	0.68	0.81	very likely	Under-consolidated
S19	Soft clay and silt	0 to 7	590	202	2.9	0.72	0.13	Almost impossible	Over-consolidated
	Greyish compacted marl	7 to 14	115	110	1.0	0.42	0.54	Moderate	Normally consolidated
	Clayey silt and soft clay	14 to 22	180	94	1.9	0.001	0.33	Impossible	Over-consolidated
S44	Muddy silt to silty sand	0 to 7	100	164	0.6	0.70	0.79	very likely	Under-consolidated
	Fine sand and silt-clay sand	7 to 14	38	64	0.6	0.001	1.00	almost certain	Under-consolidated
	Mud and soft clay	14 to 22	45	254	0.2	0.65	0.85	almost certain	Under-consolidated
S55	Silty soft clay	0 to 7	260	90	2.9	0.60	0.03	Almost impossible	Over-consolidated
	Reddish silty sand	7 to 14	260	110	2.4	0.001	0.01	Almost impossible	Over-consolidated
	Clayey sand and soft clay	14 to 22	470	92	5.1	0.55	0.00	Almost impossible	Over-consolidated

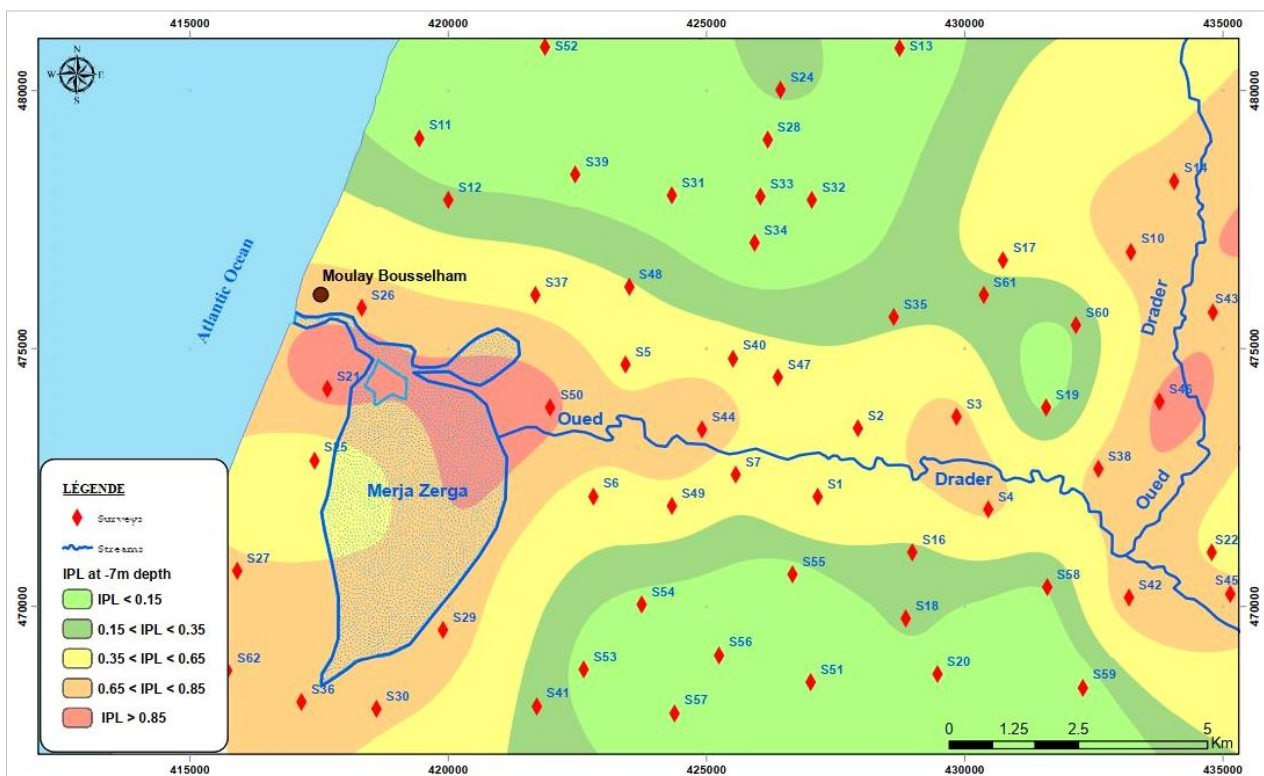


Figure 6. Map of liquefiable areas at a depth of -7 m

At a depth of -14 m (Table 5 and Figure 7), certain liquefaction is very pronounced at Marja Zerga and along the Oued Drader bed, while very probable liquefaction is widespread along the Marja Zerga and Oued Drader edges. The specific geological characteristics of this depth, the higher degree of saturation (presence of a water table), and the nature of the soil, which is sub-consolidated, seem to play a crucial role in this variation.

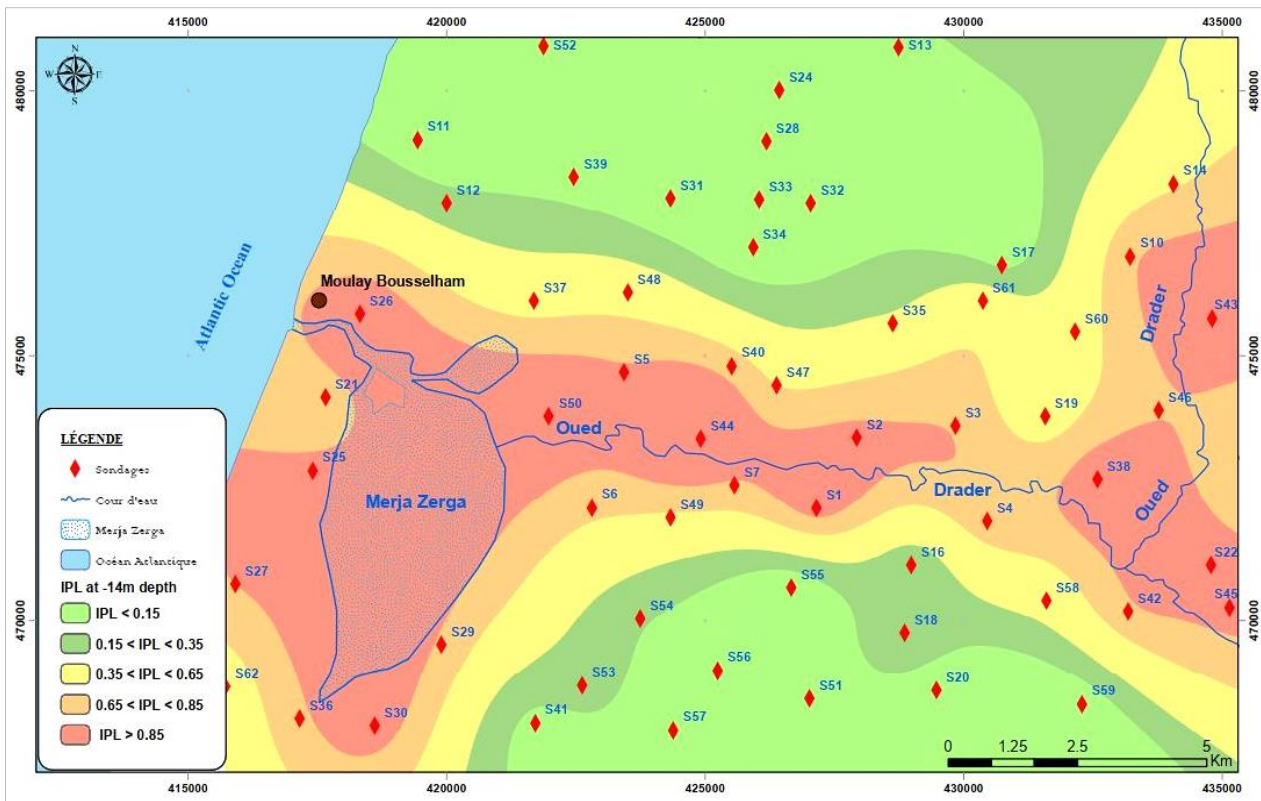


Figure 7. Map of liquefiable areas at a depth of -14 m

At a depth of -21m (Table 5 and Figure 8), certain liquefaction becomes sporadic at Oued Drader, while it becomes more pronounced at Marja Zerga. Very probable liquefaction is found along the edges of Oued Drader and Marja Zerga, suggesting that the soil lithology at this depth, combined with the presence of flood conditions, creates conditions conducive to liquefaction.

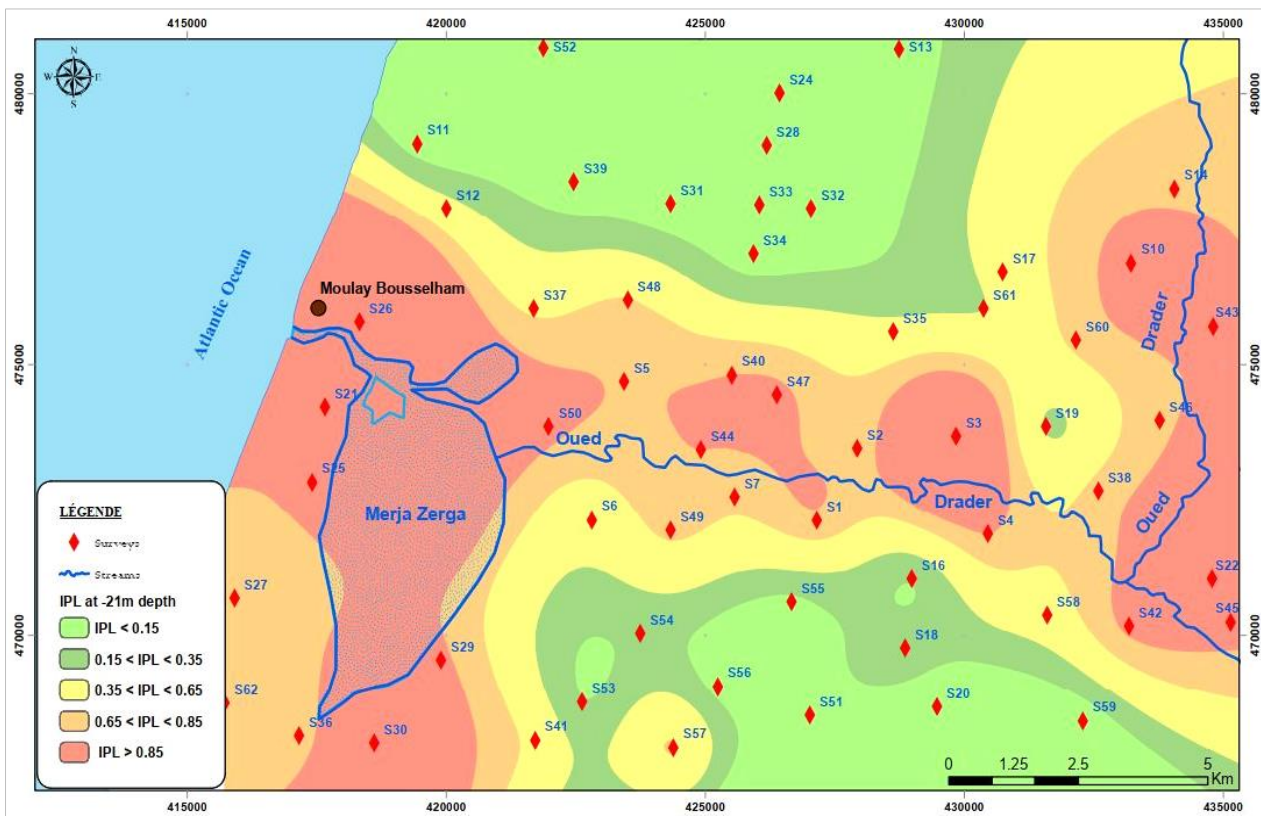


Figure 8. Map of liquefiable areas at a depth of -21 m

For drill holes located outside the alluvial and fluvial plains (Figures 6 to 8), liquefaction varies from low probability to near-impossibility due to the absence of a water table, the sandstone grading of the sediments, and the compact structure of the layers. On the other hand, we assessed susceptibility to liquefaction by calculating the over-consolidation rate for specific layers that are potentially liquefiable and for layers that are not potentially liquefiable. We found that for liquefiable layers, the over-consolidation rate indicates that the soil is under-consolidated (Table 5), and for non-liquefiable soils, it indicates that the soil is over-consolidated. This gives a result consistent with the calculation made by the semi-empirical method chosen in this study [28, 29].

The over-consolidation ratio can be used in the future to examine liquefaction potential, which is based on robust and virtually accurate laboratory results [28, 29]. The sediment slices with very probable liquefaction and certain liquefaction are found in the deposits of the Oued Drader alluvial plain and its northern and southern margins, as well as the Merja Zerga margins. These sediments, mainly composed of sands, silts, mudstones, clays, and silts, often clayey-silty or silty, are found at increasingly greater depths in the study area (Figures 6 to 8).

## 5. Conclusion

Synopsis: Analysis of the Drader River plio-quaternary complex reveals a diversity of formations: griseous, sandy, clayey, and silty. The likelihood of soil liquefaction is influenced by the frequent vertical and lateral elevations of these layers, in addition to their geomorphological characteristics. One element that encourages the liquefaction phenomenon is the existence of a phenotypic nappe.

The liquefaction index (IPL) indicates a high likelihood of liquefaction in the alluvial plain deposits of Oued Drader and Merja Zerga, with notable differences at varying depths. At -7 meters, one may observe that, in relation to Merja Zerga's proximity, liquefaction appears to have an effect, ranging from unlikely to highly possible. At -14 m, a high probability variation is due to the lithology with a high density. Liquefaction varies from low to certain at -21 m, depending on the inundation conditions and compacted lithology. This variance may be attributed to variations in the cyclic resistance calculation (CRR) as well as the fact that the degree of the earth's tremor and the presence of a phenotypic nappe have a significant influence on the determination of the liquefaction index.

The analysis suggests that the proximity to Oued Drader and Merja Zerga, as well as the presence of groundwater and the lithology of the terrain, reinforce the complexity of liquefaction. The marshy areas in the heart of Merja Zerga present a high risk, while the areas outside the alluvial deposits are more susceptible to liquefaction.

Consequently, understanding variations in liquefaction at different depths relies on a complex interplay between local geological, hydrogeological, and geotechnical characteristics. The results underline the importance of these factors in assessing liquefaction risk, providing essential data for the planning and management of potentially vulnerable areas. The over-consolidation rate method appears to be a promising approach for assessing liquefaction potential in the future, supported by robust laboratory results.

In conclusion, the Drader-Soueire basin region can be regarded as highly susceptible to liquefaction because of the earthquake risk that exists in the area as well as the type of formations in the area, which are characterized by layers of sand and silt that alternate with more clayey layers and are saturated with water due to the basin's hydrogeological nature.

## 6. Notations

<i>CSR</i>	Cyclic Stress Ratio	<i>CRR</i>	Cyclic Resistance Ratio
$\tau_{av}$	Average shear stress due to the earthquake at the depth in question	$\sigma'v0$	Effective vertical stress in (kPa)
$a_{max}$	Maximum amplitude of horizontal acceleration in (m/s <sup>2</sup> )	<i>g</i>	The acceleration of gravity = 9,81 m/s <sup>2</sup>
$\sigma v0$	Total vertical stress due to the weight of the overlying soils (kPa)	$r_d$	Stress reduction coefficient that reflects the flexibility of the soil column in (m)
<i>MSF</i>	Magnitude scaling factor	$Q_{cIN}$	The tip strength $q_c$ of the cone adjusted for stress in (kPa)
$K_f$	An intermediate parameter that was part of the regression process	$I_c$	A variable defined according to Juang and al. (2003) [4]
$F_s$	Safety factor	<i>IPL</i>	Liquefaction probability index
<i>ROC</i>	Over-consolidation ratio	$M_w$	The magnitude of the earthquake

## 7. Declarations

### 7.1. Author Contributions

Conceptualization, B.B. and A.A.; methodology, B.B., A.A., and O.E.; software, B.B.; validation, B.B. and A.A.; formal analysis, B.B. and O.E.; investigation, B.B. and O.E.; resources, B.B.; data curation, B.B. and O.E.; writing—original draft preparation, B.B., A.A., and O.E.; writing—review and editing, B.B.; visualization, B.B.; supervision, A.A.; project administration, B.B. and A.A.; funding acquisition, B.B. All authors have read and agreed to the published version of the manuscript.

## 7.2. Data Availability Statement

Data sharing is not applicable to this article.

## 7.3. Funding

The authors received no financial support for the research, authorship, and/or publication of this article.

## 7.4. Acknowledgements

We would like to express our sincere gratitude to the entire L3GIE laboratory team at Mohammadia School of Engineering.

## 7.5. Conflicts of Interest

The authors declare no conflict of interest.

## 8. References

- [1] Seed, H. B., & Idriss, I. M. (1971). Simplified Procedure for Evaluating Soil Liquefaction Potential. *Journal of the Soil Mechanics and Foundations Division*, 97(9), 1249–1273. doi:10.1061/jsfeaq.0001662.
- [2] Robertson, P. K., & Wride, C. (1998). Evaluating cyclic liquefaction potential using the cone penetration test. *Canadian Geotechnical Journal*, 35(3), 442–459. doi:10.1139/t98-017.
- [3] Idriss, I.M. and Boulanger, R.W. (2008) *Soil Liquefaction during Earthquake*. Earthquake Engineering Research Institute, Oakland, United States.
- [4] Juang, C. H., Yuan, H., Lee, D.-H., & Lin, P.-S. (2003). Simplified Cone Penetration Test-based Method for Evaluating Liquefaction Resistance of Soils. *Journal of Geotechnical and Geoenvironmental Engineering*, 129(1), 66–80. doi:10.1061/(asce)1090-0241(2003)129:1(66).
- [5] Chen, Q., Wang, C., & Hsein Juang, C. (2016). CPT-Based Evaluation of Liquefaction Potential Accounting for Soil Spatial Variability at Multiple Scales. *Journal of Geotechnical and Geoenvironmental Engineering*, 142(2), 04015077. doi:10.1061/(asce)gt.1943-5606.0001402.
- [6] Baise, L. G., Lenz, J. A., & Thompson, E. M. (2008). Discussion of “Mapping Liquefaction Potential Considering Spatial Correlations of CPT Measurements” by Chia-Nan Liu and Chien-Hsun Chen. *Journal of Geotechnical and Geoenvironmental Engineering*, 134(2), 262–263. doi:10.1061/(asce)1090-0241(2008)134:2(262).
- [7] Latifi, F. E., Baba, K., Ardouz, G., & Bouanani, L. E. L. (2023). Evaluation of Liquefaction Potential based on Cone Penetration Test (CPT) and Semi-empirical Methods. *Civil Engineering Journal (Iran)*, 9(2), 423–436. doi:10.28991/CEJ-2023-09-02-013.
- [8] Youd, T. L., & Idriss, I. M. (2001). Liquefaction Resistance of Soils: Summary Report from the 1996 NCEER and 1998 NCEER/NSF Workshops on Evaluation of Liquefaction Resistance of Soils. *Journal of Geotechnical and Geoenvironmental Engineering*, 127(4), 297–313. doi:10.1061/(asce)1090-0241(2001)127:4(297).
- [9] Lankelma G.Z. (2023). *Static Penetrometer Specialists*. Available online: <https://www.lankelma.com/> (accessed on May 2024). (In French).
- [10] Chen, C. J., & Juang, C. H. (2000). Calibration of SPT- and CPT-Based Liquefaction Evaluation Methods. *Innovations and Applications in Geotechnical Site Characterization*, 49-64. doi:10.1061/40505(285)4.
- [11] Lee, D. H., Ku, C. S., & Yuan, H. (2004). A study of the liquefaction risk potential at Yuanlin, Taiwan. *Engineering Geology*, 71(1–2), 97–117. doi:10.1016/S0013-7952(03)00128-5.
- [12] Wang, J. S., Hwang, J. H., Deng, Y. C., & Lu, C. C. (2023). Model uncertainties of SPT, CPT, and VS-based simplified methods for soil liquefaction assessment. *Bulletin of Engineering Geology and the Environment*, 82(7), 260. doi:10.1007/s10064-023-03300-6.
- [13] Toujrate, S., Baba, K., Ahatri, M., & Bahi, L. (2018). Validation and Verification of Semi-Empirical Methods for Evaluating Liquefaction Using Finite Element Method. *MATEC Web of Conferences*, 149, 02028. doi:10.1051/mateconf/201814902028.
- [14] Lunne, T., Powell, J. J. M., & Robertson, P. K. (2002). *Cone Penetration Testing in Geotechnical Practice*. CRC Press, Boca Raton, United States. doi:10.1201/978148229504.
- [15] Killi, M., El Mansouri, B., Chao, J., & et Ait Fora, A. (2007). Soil water balance and recharge of the deep-water table in the Gharb plain (Morocco). *Scientific article, Drought 2008*. 19(2), 145-151.
- [16] Aberkane, M. (1989). *Study of the Quaternary formations of the Rharrb Basin margins (northwestern Morocco)*. Thesis, University of Bordeaux, Bordeaux, France.

- [17] Haida, M., Ait Fora, A., Probst, J. L., & Snoussi, M. (1999). Hydrology and hydro-climatical fluctuations in the watershed of Sebou between 1940 and 1994. *Sécheresse*, 3(10), 221-226. (In French).
- [18] Akil, M. (1990). Quaternary coastal deposits between Casablanca and Cape Beddouza (Moroccan coastal Meseta): geomorphological and sedimentological studies. DES, Troisième cycle de Géologie. Faculté des Sciences de Rabat, Université Mohammed, 137. (In French).
- [19] Iwasaki, T., Tokida, K. I., Tatsuoka, F., Watanabe, S., Yasuda, S., & Sato, H. (1982). Microzonation for soil liquefaction potential using simplified methods. Proceedings of the 3<sup>rd</sup> international conference on microzonation, 28 June -1 July, 1982, Seattle, United States.
- [20] Puri, N., & Jain, A. (2014). Preliminary Investigation for Screening of Liquefiable areas in Haryana State, India. *ISET Journal of Earthquake Technology*, 51(1-4), 19-34.
- [21] H. Feinberg, H. (1986). The third series of the outside zones of the Rif (Maroc). *Notes et Mémoires du Service Géologique du Maroc*, 315. (In French).
- [22] Wernli, R. (1987). Neogene post-nappe micropalaeontology of northern Morocco and systematic description of planktonic foraminifera. *Service Géologique du Maroc (SGM), Rabat - Morocco*. (In French).
- [23] Erico, F. (1991). Geological and geophysical synthesis study of the Gharb basin. Report by the Office National of Petroleum Research. Rabat. Morocco.
- [24] Cherkaoui, T.E., & Asebriy, L. (2003). Seismic risk in northern Morocco Work. *Institut Scientifique, Ser. Geol. & Geogr. Phys.*, No. 21, 225-232.
- [25] Duque, J., Tafili, M., & Mašin, D. (2023). On the influence of cyclic preloads on the liquefaction resistance of sands: A numerical study. *Soil Dynamics and Earthquake Engineering*, 172, 108025. doi:10.1016/j.soildyn.2023.108025.
- [26] Idriss, I. M., & Boulanger, R. W. (2006). Semi-empirical procedures for evaluating liquefaction potential during earthquakes. *Soil Dynamics and Earthquake Engineering*, 26(2-4 SPEC. ISS.), 115-130. doi:10.1016/j.soildyn.2004.11.023.
- [27] S Liao, S.S.C. and Whitman, R.V. (1986) Catalogue of Liquefaction and Non-Liquefaction Occurrences during Earthquakes. Report, Department of Civil Engineering, Massachusetts Institute of Technology, Cambridge, United States.
- [28] Nagase, H., Shimizu, K., Hiro-Oka, A., Mochinaga, S., & Ohta, M. (2000). Effects of over consolidation on liquefaction strength of sandy soil samples. Proceedings of 12<sup>th</sup> world conference on earthquake engineering, 30 January - Friday 4, Auckland, New Zealand.
- [29] Mahmoudi, Y., Cherif Taiba, A., Hazout, L., Belkhatir, M., & Baille, W. (2020). Packing Density and Overconsolidation Ratio Effects on the Mechanical Response of Granular Soils. *Geotechnical and Geological Engineering*, 38(1), 723-742. doi:10.1007/s10706-019-01061-2.